Appl. Phys. B 35, 217–225 (1984)

Applied Physics B Photophysics and Laser Chemistry

Using the Seventh-Order Numerical Method to Solve First-Order Nonlinear Coupled-Wave Equations for Degenerate Two-Wave and Four-Wave Mixing

Y. H. Ja

Telecom Australia, Research Laboratories, Box 249, Clayton North 3168, Australia

Received 28 May 1984/Accepted 28 July 1984

Abstract. Using a new seventh-order numerical method [the $O(h^7)$ method] for solving two-point boundary value problems, numerical solutions of the first-order nonlinear coupled-wave equations for degenerate two-wave and four-wave mixing in a reflection geometry have been obtained. A computer program employing the Gauss-Jordan elimination technique has also been adopted to effectively solve the resultant large, sparse and unsymmetric matrix, obtained from the $O(h^7)$ method and the Newton-Raphson iteration method. Numerical results from the computer calculations are presented graphically. A comparison between this $O(h^7)$ method and the shooting method, mainly from the viewpoint of computational efficiency, is also made.

PACS: 42.65, 78.20

Owing to the great promise for many practical applications, such as real-time optical information processing and adaptive optics, degenerate four-wave mixing (DFWM) and its closely related field, degenerate two-wave mixing (DTWM), using photorefractive crystals as nonlinear media, have attracted much attention in recent years [1]. Some of the the photorefractive crystals such as $LiNbO_3$, have been used as the recording media in conventional holography for sometime already [2].

A task of major importance in DTWM and DFWM is to solve the first-order nonlinear coupled-wave equation (which is obtained by using the slowly varying envelope approximation (SVEA) [3, 4]) and to obtain the resultant intensity of the signal beam (in DTWM) or the wavefront reflectivity (in DFWM). Due to the mathematical complexity in general, only approximate analytical solutions (which may not be derived from the nonlinear coupled-wave equations) or exact numerical solutions can be obtained under assumptions of special conditions. These assumptions have included low beam-coupling, low diffraction efficiency [5, 6], nondepleting pump beams [7] and a nonabsorbing medium [8]. To gain a better understanding of DTWM and DFWM, it is necessary to obtain accurate solutions of these nonlinear equations under more general conditions.

In [9–11], we have used the shooting method (one of the numerical methods to solve two-point boundary-value problems) to obtain accurate numerical solutions of the first-order nonlinear coupled-wave equations for DTWM and DFWM. No special conditions, such as those mentioned above, need be assumed.

In this paper, we use a new seventh-order numerical method [the $O(h^7)$ method] [12], to obtain the numerical solutions of the nonlinear equations for DTWM and DFWM in a reflection geometry. Although this $O(h^7)$ method differs from the simple finite difference method, it may still be considered as one of the finite difference methods [13].

As before [9–11], throughout this paper only are the steady-state solutions of the nonlinear equations for DTWM and DFWM at saturation stage sought. This means that the solution is time independent and the relevant parameter, such as the effective coupling constant g, see what follows (14 and 18), is independent of incident beam intensities. Saturation of g occurs when the trapping centres in the crystal are completely

filled with the photoinduced charge carriers. This occurs only at a relatively high power density of incident beams.

In the following, we first describe Tewarson's seventh-order numerical method [12]. This method and the Newton-Raphson iteration method [13] are then used to derive the coefficient matrix from the corresponding first-order nonlinear coupled-wave equations for DTWM and DFWM, respectively. Next we give a brief description of Key's computer program [14] which is very effective in solving the resultant large, sparse and unsymmetric matrix, using the Gauss-Jordan elimination and special pivot selecting schemes.

Computed results will be presented in graphical form. Finally, a comparison is made between the shooting method [9, 10, 13] and the $O(h^7)$ method used here.

1. The Seventh-Order Numerical Method

1.1. General Description of the $O(h^7)$ Method

Very recently, Tewarson reported [12] a new method for the numerical solution of two-point boundary value problems for first-order nonlinear ordinary differential equations. This method has a higher-order accuracy [of order $O(h^7)$, where h is the space step size], than many other numerical methods. Furthermore, this increased accuracy is achieved with no increase in computation time, because less function evaluations are required for each sub-interval.

Adopting the approach of Tewarson [12], let us consider the following systems of first-order differential equations

$$\bar{y}'(z)=\bar{f}(z,\bar{y}(z)), \tag{1}$$

with the two-point boundary conditions

$$\bar{g}(\bar{y}(0),\bar{y}(1))=0, \tag{2}$$

where $\bar{f}$, $\bar{g}$, and $\bar{y}$ are m-vectors, $\bar{y}'$ is the first-order derivative of function $\bar{y}$ with respect to z, which is the independent variable and is normalized, i.e. $0\leqq z\leqq 1$.

This range of z is subdivided into n equal parts with $h=1/n$ and $z_i=ih$, $i=0,1,\ldots,n$. Then integrating the p^{th} equation of (1) in the interval $[z_{i-1}, z_i]$, yields the residual quantity

$$\phi_{p,i}(\bar{y})=y_{p,i}-y_{p,i-1}-\int_{z_{i-1}}^{z_i} f_p(z,\bar{y}(z))dz=0, \tag{3}$$

where $y_{p,i}=y_p(z_i)$ and $p=1,2,\ldots,m$.

Using the $O(h^7)$ method [12], we obtain

$$\int_{z_{i-1}}^{z_i} f_p(z,\bar{y}(z))dz=\frac{7h}{30}(f_{p,i-1}+f_{p,i})+\frac{8h}{15}f_{p,i-1/2}+\frac{h^2}{60}(f^1_{p,i-1}-f^1_{p,i})+O(h^7), \tag{4}$$

where $O(h^7)$ denotes an error term in the order of h^7,

$$f_{p,i}=f_p(z_i,\bar{y}(z_i)), \tag{5}$$

$$f_{p,i-1/2}=f_p\left(z_i-\frac{h}{2},\bar{y}\left(z_i-\frac{h}{2}\right)\right) \tag{6}$$

and

$$y_{p,i-1/2}=(y_{p,i-1}+y_{p,i})/2+(5h/32)(f_{p,i-1}-f_{p,i})+(h^2/64)(f^1_{p,i-1}+f^1_{p,i}). \tag{7}$$

The terms $f^1_{p,i-1}$ and $f^1_{p,i}$ represent first derivatives of f_p and can be obtained from (1) as follows

$$f^1_p=\frac{\partial f_p}{\partial z}+\frac{\partial f_p}{\partial \bar{y}}\cdot\frac{\partial \bar{y}}{\partial z}=\frac{\partial f_p}{\partial z}+\frac{\partial f_p}{\partial \bar{y}}\cdot\bar{f}. \tag{8}$$

Finally, neglecting the error term $O(h^7)$ in (4), (3) becomes

$$\bar{\phi}(\bar{y})=0, \tag{9}$$

where $\bar{\phi}$ denotes a vector with the components $\phi_{p,i}$.

In (2) we assume that $\bar{g}$ is a linear function of $\bar{y}$, and consequently m components of $\bar{y}$ in (9) have been eliminated by expressing them as linear functions of other components of $\bar{y}$, using the boundary conditions (2) [12].

Note that in (4) only $f^1_{p,i-1}$ and $f^1_{p,i}$ are needed. The additional terms $f^2_{p,i-1}$ and $f^2_{p,i}$ (the second derivatives) as required in another method [15], are not necessary and therefore the computation time is reduced.

1.2. Resultant Matrix Equation for DTWM

From the discussion in Sect. 1.1, the main problem is to determine a solution to (9). Since the Newton-Raphson iteration method usually converges faster than most other methods, we use it to solve $\bar{\phi}(\bar{y})=0$.

The modified Newton-Raphson iteration method [13] for solving $\bar{\phi}(\bar{y})=0$ is

$$\bar{y}^{(t+1)}=\bar{y}^{(t)}+\omega_t\delta\bar{y}^{(t)}, \tag{10}$$

where

$$\bar{J}(\bar{y}^{(t)})\delta\bar{y}^{(t)}=-\bar{\phi}(\bar{y}^{(t)}) \tag{11}$$

assuming the Jacobian matrix $\bar{J}(\bar{y})=[\partial\phi_{p,i}/\partial y_j]$ is non-singular, and $\omega_t\leqq 1$. This is chosen to ensure that

$$|\bar{\phi}(\bar{y}^{(t+1)})|<|\bar{\phi}(\bar{y}^{(t)})|. \tag{12}$$

The elements of the Jacobian matrix $\bar{J}$ can be approximated [13] as

$$\frac{\partial\phi_{p,i}}{\partial y_j}\cong\frac{\phi_{p,i}(y_j+\delta y_j)-\phi_{p,i}(y_j)}{\delta y_j}. \tag{13}$$

Now (11) can be constructed, using the nonlinear coupled-wave equations for DTWM and (3–8), given by the $O(h^7)$ method.

The construction of this type of equation is tedious, especially for the case fo four-wave mixing or $N(>4)$-wave mixing. Therefore only a brief description of the procedure is presented.

For DTWM in a reflection geometry without an applied electric field and ignoring the boundary reflection components, the first-order nonlinear coupled-wave equations are given as follows [9]

$$\left.\begin{aligned}\frac{dy_1}{dz} &= -\alpha l y_1 - 2gl\frac{y_1 y_2}{y_1+y_2} = f_1\\ \frac{dy_2}{dz} &= \alpha l y_2 - 2gl\frac{y_1 y_2}{y_1+y_2} = f_2\end{aligned}\right\}, \tag{14}$$

$$\alpha = \alpha_i/\cos\theta_n,$$

$$g = \frac{\pi n_0^3 r E_T}{(\lambda\cos\theta_n)(1+E_T/E_q)},$$

$$E_T = 2\pi k_B T/(e\Lambda) = A/\Lambda, \tag{15}$$

$$E_q = \frac{eN\Lambda}{2\pi\varepsilon_0\varepsilon_r} = B\Lambda,$$

$$\Lambda = \frac{\lambda}{2n_0\cos\theta_n}.$$

In the above y_1 and y_2 are the intensities of the two plane waves $\bar{A}_1$ and $\bar{A}_2$, respectively, α_i is the intensity absorption coefficient of the nonlinear medium at the operating wavelength λ and g is the effective coupling constant [7, 9]. E_T is the diffusion field, E_q is the maximal field of the volume space-charge field, n_0 is the average refractive index of the medium, r is the appropriate electro-optic coefficient of the medium, k_B is Boltzmann's constant, T is the temperature, e is the electronic charge, Λ is the fringe spacing, $\varepsilon\,(=\varepsilon_0\varepsilon_r)$ is the static dielectric constant of the medium, N is the concentration of trapping centres, l is the thickness of the medium, and θ_n is the internal angle between the beams and the axis z' (Fig. 1a). In (14), $z\ (=z'/l)$ is normalized (from 0 to 1).

Using (8 and 14), we obtain

$$\begin{aligned}f_1' &= \frac{\partial f_1}{\partial z} + \frac{\partial f_1}{\partial \bar{y}}\frac{\partial \bar{y}}{\partial z} = \frac{\partial f_1}{\partial y_1}\frac{\partial y_1}{\partial z} + \frac{\partial f_1}{\partial y_2}\frac{\partial y_2}{\partial z}\\ &= \left(-\alpha l - 2gl\frac{y_2^2}{(y_1+y_2)^2}\right) f_1\\ &\quad - 2gl\frac{y_1^2}{(y_1+y_2)^2} f_2.\end{aligned} \tag{16}$$

Similarly we have

$$\begin{aligned}f_2' &= -2gl\frac{y_2^2}{(y_1+y_2)^2} f_1\\ &\quad + \left(-\alpha l - 2gl\frac{y_1^2}{(y_1+y_2)^2}\right) f_2.\end{aligned} \tag{17}$$

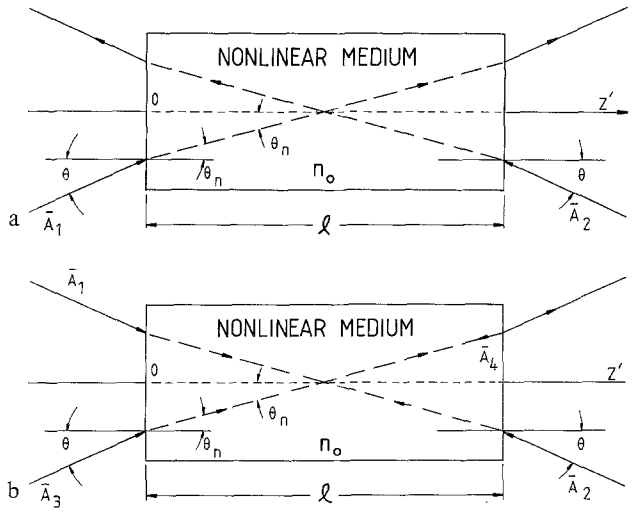

Fig. 1a and b. The configurations of (a) degenerate two-wave mixing and (b) degenerate four-wave mixing in a reflection geometry. The average refractive index of the nonlinear medium $n_0 > 1$ is shown

From (3, 4, 16, and 17), one can see that $\phi_{p,i}(\bar{y})$ does not depend on every component of $\bar{y}$, therefore the Jacobian matrix $\bar{J}(\bar{y}) = [\partial\phi_{p,i}/y_j]$ [i.e., the coefficient matrix in (11)] contains many zero elements and is a sparse matrix [14].

1.3. Resultant Matrix Equation for DFWM

The matrix equation for DFWM can be derived in a similar way to the case of DTWM, although the procedure is more complex. For DFWM in a reflection geometry with applied electric field $E_0 = 0$ and neglecting the boundary reflection components, the first-order nonlinear coupled-wave equations are as follows [7, 10]

$$\begin{aligned}\frac{dy_1}{dz} &= f_1 = -\alpha l y_1 - 2gl\frac{y_1 y_4 \pm (y_1 y_2 y_3 y_4)^{1/2}}{y_0},\\ \frac{dy_2}{dz} &= f_2 = \alpha l y_2 - 2gl\frac{y_2 y_3 \pm (y_1 y_2 y_3 y_4)^{1/2}}{y_0},\\ \frac{dy_3}{dz} &= f_3 = -\alpha l y_3 - 2gl\frac{y_2 y_3 \pm (y_1 y_2 y_3 y_4)^{1/2}}{y_0},\\ \frac{dy_4}{dz} &= f_4 = \alpha l y_4 - 2gl\frac{y_1 y_4 \pm (y_1 y_2 y_3 y_4)^{1/2}}{y_0}.\end{aligned} \tag{18}$$

Here y_1, y_2, y_3, and y_4 are the intensities of two antipropagating pump beams $\bar{A}_1$ and $\bar{A}_2$, the signal and the generated phase-conjugate beams $\bar{A}_3$ and $\bar{A}_4$, respectively, as shown in Fig. 1b. Then $y_0 = y_1 + y_2 + y_3 + y_4$ is the total beam intensity. The $(+)$ sign in (18) applies for $g > 0$ while the $(-)$ sign applies for $g < 0$ [7]. Other parameters have been defined previously.

Using (8 and 18), we have

$$
\begin{aligned}
f_1' &= \frac{\partial f_1}{\partial y_1} f_1 + \frac{\partial f_1}{\partial y_2} f_2 + \frac{\partial f_1}{\partial y_3} f_3 + \frac{\partial f_1}{\partial y_4} f_4, \\
f_2' &= \frac{\partial f_2}{\partial y_1} f_1 + \frac{\partial f_2}{\partial y_2} f_2 + \frac{\partial f_2}{\partial y_3} f_3 + \frac{\partial f_2}{\partial y_4} f_4, \\
f_3' &= -\alpha l(f_2 + f_3) + f_2', \\
f_4' &= \alpha l(f_1 + f_4) + f_1',
\end{aligned}
\tag{19}
$$

where

$$
\begin{aligned}
\frac{\partial f_1}{\partial y_1} &= -\alpha l - 2gl \frac{[y_4 \pm \tfrac{1}{2}(y_1y_2y_3y_4)^{-1/2} y_2y_3y_4] y_0 - [y_1y_4 \pm (y_1y_2y_3y_4)^{1/2}]}{y_0^2}, \\
\frac{\partial f_1}{\partial y_2} &= -2gl \frac{[\pm \tfrac{1}{2}(y_1y_2y_3y_4)^{-1/2} y_1y_3y_4] y_0 - [y_1y_4 \pm (y_1y_2y_3y_4)^{1/2}]}{y_0^2}, \\
\frac{\partial f_1}{\partial y_3} &= -2gl \frac{[\pm \tfrac{1}{2}(y_1y_2y_3y_4)^{-1/2} y_1y_2y_4] y_0 - [y_1y_4 \pm (y_1y_2y_3y_4)^{1/2}]}{y_0^2}, \\
\frac{\partial f_1}{\partial y_4} &= -2gl \frac{[y_1 \pm \tfrac{1}{2}(y_1y_2y_3y_4)^{-1/2} y_1y_2y_3] y_0 - [y_1y_4 \pm (y_1y_2y_3y_4)^{1/2}]}{y_0^2}, \\
\frac{\partial f_2}{\partial y_1} &= -2gl \frac{[\pm \tfrac{1}{2}(y_1y_2y_3y_4)^{-1/2} y_2y_3y_4] y_0 - [y_2y_3 \pm (y_1y_2y_3y_4)^{1/2}]}{y_0^2},
\end{aligned}
\tag{20}
$$

$$
\begin{aligned}
\frac{\partial f_2}{\partial y_2} &= \alpha l - 2gl \frac{[y_3 \pm \tfrac{1}{2}(y_1y_2y_3y_4)^{-1/2} y_1y_3y_4] y_0 - [y_2y_3 \pm (y_1y_2y_3y_4)^{1/2}]}{y_0^2}, \\
\frac{\partial f_2}{\partial y_3} &= -2gl \frac{[y_2 \pm \tfrac{1}{2}(y_1y_2y_3y_4)^{-1/2} y_1y_2y_4] y_0 - [y_2y_3 \pm (y_1y_1y_3y_4)^{1/2}]}{y_0^2}, \\
\frac{\partial f_2}{\partial y_4} &= -2gl \frac{[\pm \tfrac{1}{2}(y_1y_2y_3y_4)^{-1/2} y_1y_2y_3] y_0 - [y_2y_3 \pm (y_1y_2y_3y_4)^{1/2}]}{y_0^2}.
\end{aligned}
\tag{21}
$$

The resultant $4n \times 4n$ coefficient matrix $\bar{J}(\bar{y})$ for DFWM then has the following form

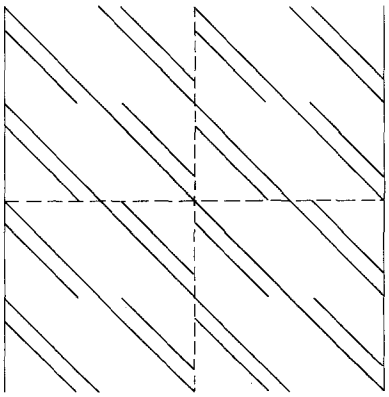

(22)

where the blanks denote zero elements. The longer straight lines denote diagonal or sub-diagonal non-zero elements and the shorter lines denote non-diagonal non-zero elements which are adjacent to the corresponding diagonal or sub-diagonal elements. Note that the coefficient matrix $\bar{J}(\bar{y})$ in (11) for DTWM has the same shape as the upper-left quarter matrix in (22), although the values of the corresponding elements are different.

2. Computer Program for Solving Matrix Equation with a Large, Sparse, Unsymmetric, and Banded Coefficient Matrix

An inspection of (22) indicates that the coefficient matrix is an unsymmetric, banded and sparse matrix, whose band-width ($=n+2$ and $3n+2$ for DTWM and DFWM, respectively) is not very narrow and increases with the number of the sub-interval n.

There are numbers of different techniques to diagonalize such a matrix, and consequently to obtain the solution of the corresponding equation. Here we adopt Key's computer program in which the Gauss-Jordan elimination technique is employed, and a pivotal element selection scheme is incorporated. The latter reduces computer storage and computation time and allows reasonably accurate results to be obtained [14]. The Gauss-Jordan elimination technique has been proven to be more effective than the Gauss elimination technique for solving large matrices [14].

The details of this computer program have been described elsewhere [14] and will not be discussed here. A unique feature of this computer program is its storage scheme in which two arrays are needed. One array contains the non-zero elements of the coefficient matrix while the other contains the column index of the corresponding elements. For a sparse matrix having say $n>30$, the saving in computer storage is obvious.

Our study shows that, as reported by Key [14], the minimum row-minimum column pivot selection scheme is also the best of several possible pivot selection schemes for solving the first-order nonlinear equations for DTWM and DFWM. This is judged from the accuracy of the computer results, computation time, total number of terms removed in the elimination process and the maximum number of columns of storage required during the solution process. However, in our case, the differences in computer time and accuracy of results obtained when using different pivot selection schemes are not so dramatic as reported previously [14]. In this paper, we therefore present the computed results obtained by using the minimum row-minimum column pivot selection scheme only.

3. Computed Results and Discussion

3.1. Computed Results of DTWM

In this subsection the matrix form of (11) for DTWM will be solved using the Gauss-Jordan elimination scheme and the minimum row-minimum column pivot selection scheme [14]. Since major results have been obtained and reported by using the direct numerical method [16] and the shooting method [9], we compute only the dependence of the so-called effective gain γ_0 [17] on the external incident angle θ, (made between the incident beam and the axis z', Fig. 1a), on the operating wavelength λ and on the gain factor gl.
The effective gain [17] is defined as

$$\gamma_0 = \frac{y_2 \text{ with reference beam}}{y_2 \text{ without reference beam}} = \frac{y_2(0)|_g}{y_2(0)|_{g=0}}. \tag{23}$$

It is obvious from (14, 15, and 23) that there is complex dependence of γ_0 on the gain factor gl, on the incident angle θ, and on the operating wavelength λ, respectively.
In solving the matrix equation (11) using our computer program, the starting value of $\bar{y}$ ($y_{p,i}$ where $p=1, 2$, and $i=1, 2, \ldots, n+1$) is chosen as a vector of all unities or other integral numbers [except at the boundary where the value is given by the boundary condition $M=_{2,n+1}(I)/y_{1,1}(0)$, and $y_{1,1}(0)$ is normalized to one]. Convergence was reached in only several iterations.
The intensity absorption coefficient α_i of a photorefractive crystal depends on the operating wavelength λ and usually decreases with an increasing wavelength. However, the relation between α_i and λ, and the value of α_i are different for different types of photorefractive crystals. Thus in our computation, we use the following approximate relation between α_i and λ;

$$\alpha_i(\lambda) = \frac{C \cdot 10^{-9}\,\text{cm}}{\lambda^2}, \tag{24}$$

where C is a dimensionless constant.
Note that (24) is only valid inside the transparent region of the crystal (say $\lambda=0.45$ to 7.5 μm for BGO [18]). The shape of the curve of α_i against λ obtained from (24) is similar to that of the measured curve for BGO [19].
Figures 2a–c show the computed dependence of the effective gain γ_0 on the incident angle θ with the initial beam intensity ratio M, the intensity absorption coefficient α_i, and the refractive index of the nonlinear medium n_0, as parameter, respectively. Inspection of Fig. 2 indicates the following
1) For a large n_0 (say $n_0=2.5$) γ_0 increases only slightly with θ and the relation between γ_0 and θ is approximately linear. However, for a small n_0 (Fig. 2c) γ_0 increases significantly with θ, and the relation between γ_0 and θ is nonlinear.
2) γ_0 increases rapidly with n_0 (Fig. 2c).
The computed curves of the effective gain γ_0 against the operating wavelength λ, with the initial beam ratio M, the intensity absorption coefficient α_i and the refractive index n_0 as a parameter are shown in Fig. 3a–c, respectively. Here the slight variation of the refractive index n_0 with the operating wavelength λ is ignored. It can be seen from these figures that the relationship of γ_0 to λ is approximately linear and that γ_0 changes very little with λ, for λ ranging from 0.45 to 0.75 μm. The reason is that although α_i decreases with λ, (24), γ_0 has a weak dependence on α or α_i (Fig. 2b) and that the effective coupling constant g only changes slightly with spatial frequency or λ [20, 21]. The dependence of γ_0 on other parameters such as M, α_i, and n_0 is similar to that shown in Fig. 2a–c.
The relation between the effective gain γ_0 and the gain factor gl is computed and shown in Fig. 4. Inspection of this figure indicates the following characteristics
1) The dependence of γ_0 on gl is nonlinear, and γ_0 increases rapidly with gl.
2) The rate of change of γ_0 with gl increases with decreasing M.
There is some complexity when using θ or λ as the independent variable since g and α both depend on θ and λ, (15 and 24). Therefore in some cases, an appropriate interpretation may be difficult.

3.2. Computed Results of DFWM

As in the case of DTWM, the matrix equation for DFWM is constructed using (11 and 18–21), and then

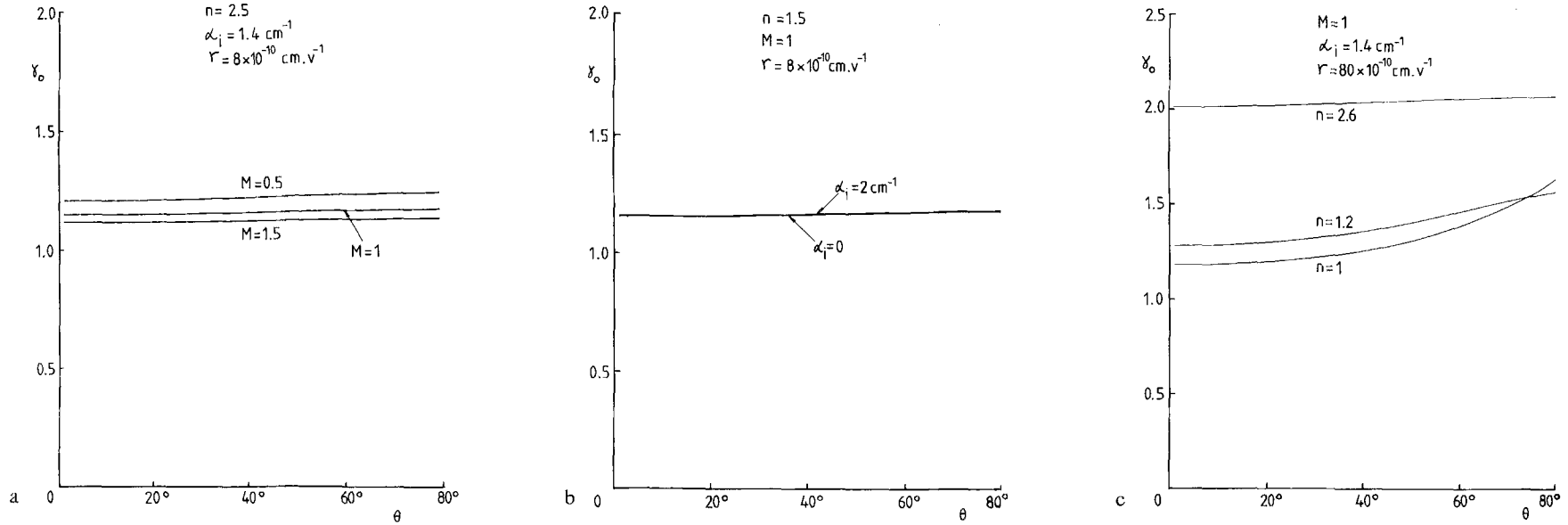

Fig. 2a–c. Computed curves of effective gain γ_0 against incident angle θ in two-wave mixing with (a) initial beam-intensity ratio $M = y_2(l)/y_1(0)$, (b) intensity absorption coefficient, α_i, and (c) the average refractive index of the nonlinear medium n_0, as a parameter, respectively. Operating wavelength $\lambda = 0.5\,\mu m$, field parameters $A = 0.16\,V$, $B = 1 \times 10^8\,V\,cm^{-2}$ and medium thickness $l = 0.2\,cm$

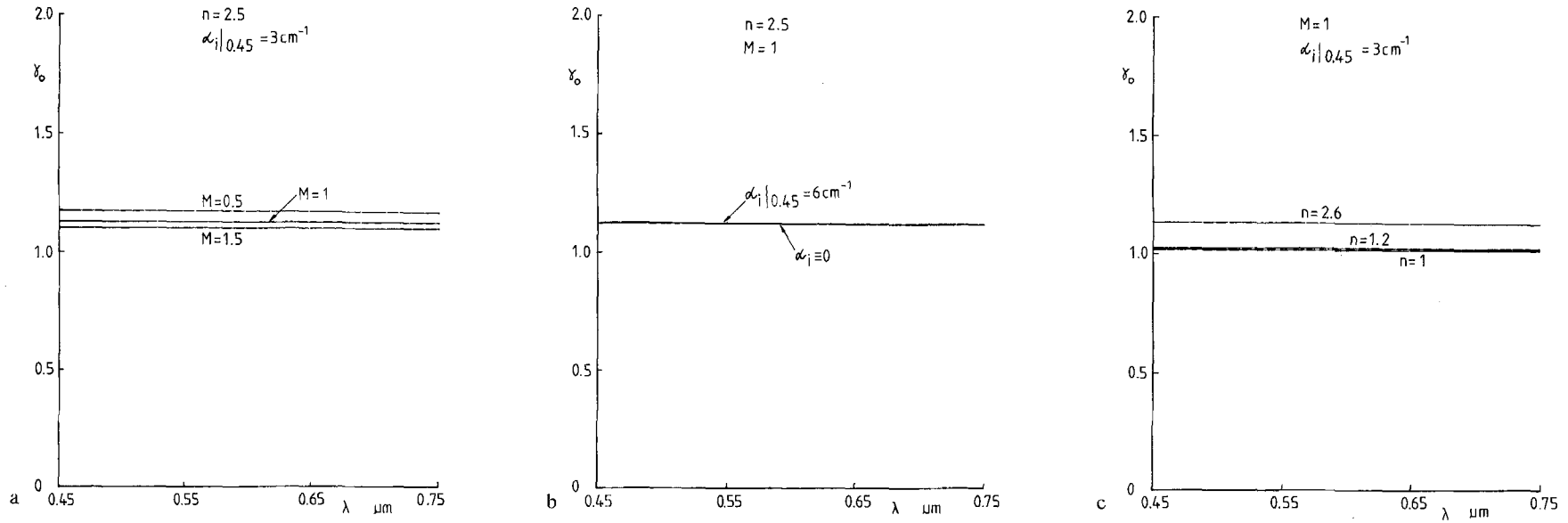

Fig. 3a–c. Computed curves of effective gain γ_0 against operating wavelength λ in two-wave mixing with (a) initial beam-intensity ratio $M = y_2(l)/y_1(0)$, (b) intensity absorption coefficient α_i, and (c) the average refractive index of the nonlinear medium n_0 as a parameter, respectively. Incident angle $\theta = 20°$, field parameter $B = 0.8 \times 10^8\,V\,cm^{-2}$, and electro-optic coefficient $r = 8 \times 10^{-10}\,V\,cm^{-1}$. Other parameters are the same as those in Fig. 2

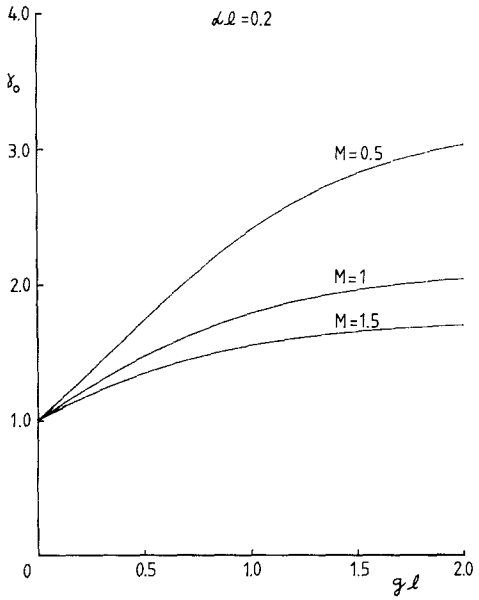

Fig. 4. Computed dependence of effective gain γ_0 on gain factor gl in two-wave mixing with initial beam-intensity ratio $M = y_2(l)/y_1(0)$ as a parameter

is solved using Key's program. For the same total number of the sub-interval n, the size of the matrix for DFWM is four times that for DTWM, so that more computing time will be required.

Here, we only compute the dependence of wavefront reflectivity W ($= y_4(0)/y_3(0)$, the intensity ratio of the generated phase-conjugate beam to the object beam at $z=0$) on the incident angle θ and on the attenuation factor αl. These results have not been computed and reported previously. Figure 5a–d show the calculated dependence of W on θ with the initial pump beam ratio $r_p = y_2(l)/y_1(0)$, the reference-to-object beam ratio $M_1^{-1} = y_2(l)/y_3(0)$, the intensity absorption coefficient α_i at the operating wavelength λ and the refractive index of the nonlinear medium n_0 as a parameter, respectively.

An examination of Fig. 5a–d shows the following characteristics:

1) Generally, the relationship between the wavefront reflectivity W and the external incident angle θ is nonlinear.

2) In Fig. 5a–c where an artificial refractive index $n_0 = 1$ is assumed (which is of theoretical interest only, for in practice such a nonlinear medium does not exist), W at first increases slowly then rapidly with θ, reaches a maximum at about 70–80° and then decreases with θ. This is because both the gain factor gl and the attenuation factor αl increase with θ, (15). The former tends to increase W, while the latter tends to decrease W. At a smaller θ, the increase of gl with θ is faster than that of αl. The net result is therefore the increase of W with θ. However, when θ approaches 90° the attenuation factor αl is dominant and this results in the decrease of W with θ. The position of the maximum of W depends on the material and geometrical parameters. For example, in Fig. 5c, the position of the maximum moves towards a smaller θ when α_i increases. When $\alpha_i = 0$, no maximum of W exists.

3) For $n_0 \neq 1$, i.e. in a practical case, there is no maximum in the curves of W against θ (Fig. 5d). This is probably due to the fact that the corresponding change of the Bragg angle θ_n inside the medium is much less than that of the external incident angle θ which changes from about 0° to 80°. In consequence, the variations of gl and αl (esecially the latter) will not be so dramatic as in the case of $n_0 = 1$.

4) When $n_0 \neq 1$, the reflection at the surface of the medium has to be considered. In this case the wavefront reflectivity W outside the medium should be the product of the wavefront reflectivity calculated directly by solving the matrix equation for DFWM and the factor $(1-R)^2$, where R is the intensity reflection coefficient. R depends on the incident angle θ and the polarization of the beam and usually increases rapidly with θ. In Fig. 5d, the curves of the actual wavefront reflectivity $W' = (1-R)^2 W$ plotted against θ are also presented, where vertical polarization of the beams has been assumed. The curves of W' against θ show the angular response or the spatial frequency response of the DFWM. From Fig. 5d, it is obvious that W' decreases significantly at larger θ. Note that the curve of W' against θ will be flatter and that the value of W' increases at a small θ when n_0 increases, while the spatial frequency response becomes narrower. The curve of W' against θ for $n_0 = 1$ is also plotted for comparison.

Figure 6 shows the computed relation between W and the attenuation factor αl. Evidently the relation is nonlinear and W decreases rapidly with αl.

3.3. Comparison Between the $O(h^7)$ Method and the Shooting Method

The computed results in this paper and in [9–11] indicate that both the $O(h^7)$ method and the shooting method are well suited to solving the first-order nonlinear coupled-wave equations for DTWM and DFWM. A comparison between these two methods shows the following points:

1) The shooting method is more straightforward, is easier to program in a general form, and easier to handle than the $O(h^7)$ method. This is because in the $O(h^7)$ method the process of setting up the (usually

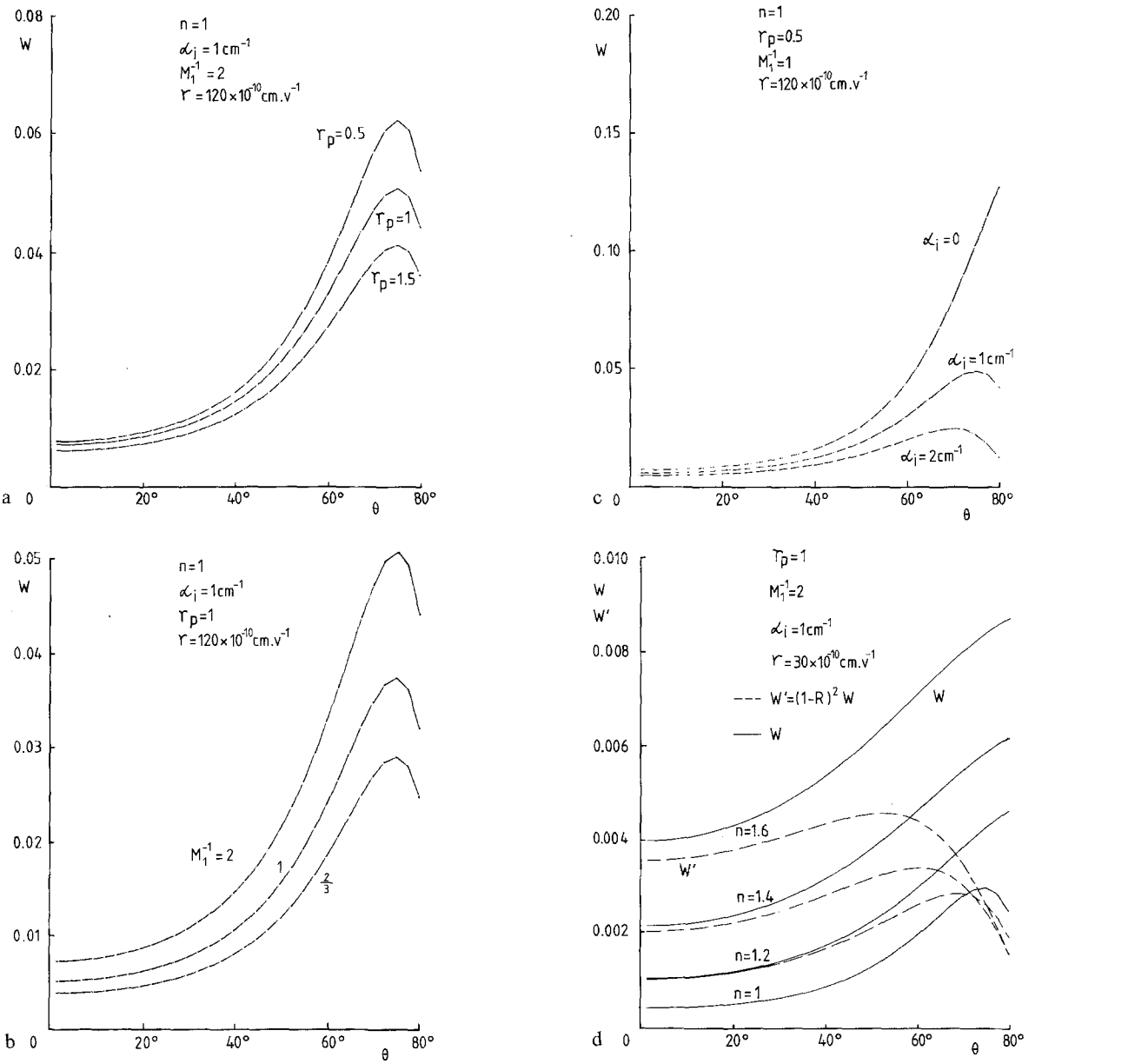

Fig. 5a–d. Computed dependence of wavefront reflectivity W on incident angle θ in four-wave mixing with (a) initial pump intensity ratio $r_p = y_2(l)/y_1(0)$, (b) reference-to-object beam ratio $M_1^{-1} = y_2(l)/y_3(0)$, (c) intensity absorption coefficient α_i, and (d) the average refractive index of the nonlinear medium n_0 as a parameter, respectively. In (d), the computed curves of actual wavefront reflectivity $W' = (1-R)^2 W$ against θ are also shown. Field parameters $A = 0.16\,V$, $B = 0.8\times10^8\,V\,cm^{-2}$, operating wavelength $\lambda = 0.5\,\mu m$ and medium thickness $l = 0.2\,cm$

large) matrix is rather involved, and a complex storage scheme such as that used in [2] has to be used in order to save storage and computing time.

2) In the $O(h^7)$ method, the starting values of the solution over the whole range have to be guessed while in the shooting method, only a few boundary values need be estimated. This places a more rigid constraint on the starting values for the $O(h^7)$ method. In our computation using the $O(h^7)$ method it has been found that in some cases a starting matrix of the solution with all elements being unity does not work. The values of the elements have to be much larger than unity.

3) To obtain the same accuracy in computed results, the $O(h^7)$ method is generally faster than the shooting method in computing time. Furthermore, for a moderate accuracy (say, the relative error is $10^{-3} \sim 10^{-4}$), a coarse space-meshing (i.e., a small n, say $8 \sim 10$) can be used in the $O(h^7)$ method.

4) Considerable storage capacity is usually required for the $O(h^7)$ method even when special storage

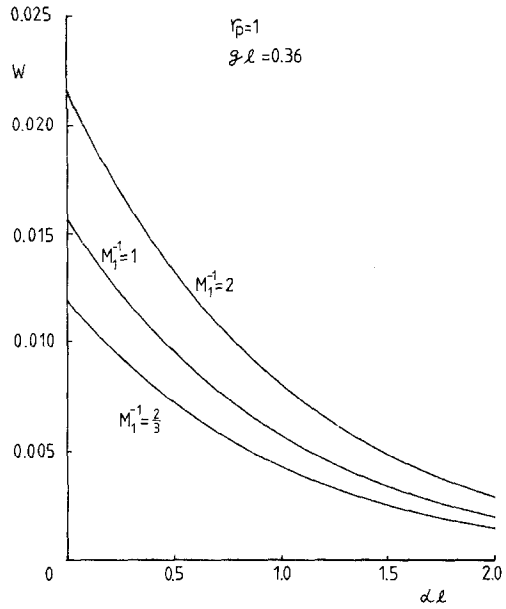

Fig. 6. Computed relation between wavefront reflectivity W and attenuation factor αl in four-wave mixing with reference-to-object beam ratio $M_1^{-1}=y_2(l)/y_3(0)$ as a parameter

schemes [14] have been used, whereas storage is not a problem in the shooting method.

4. Conclusions

The seventh-order numerical method [12] for solving two-point boundary-value problems, has been used to obtain numerical solutions of the first-order nonlinear coupled-wave equations for DTWM and DFWM. This method usually uses less computer time than the shooting method [9, 10, 13], although more storage is required. Also there is some difficulty in using it as a basis for a general routine and in automatic computation.

Acknowledgements. I wish to thank Drs. P. V. H. Sabine and G. Stone for useful discussions. The permission of the Director, Research Laboratories, Telecom Australia, to publish this paper is acknowledged.

References

1. J. Feinberg: In *Optical Phase Conjugation*, ed. by R.A. Fisher (Academic Press, New York 1983) pp. 417–443
2. E.G. Ramberg: RCA Rev. **33**, 5–53 (1972)
3. H. Kogelnik: Bell Syst. Tech. J. **48**, 2909–2947 (1969)
4. A. Yariv, R.A. Fisher: In *Optical Phase Conjugation*, ed. by R.A. Fisher (Academic Press, New York 1983) pp. 9–11
5. J.P. Huignard, J.P. Herriaue, G. Rivet, P. Gunter: Opt. Lett. **5**, 102–105 (1980)
6. Y.H. Ja: Opt. Commun. **41**, 159–163 (1982)
7. N.V. Kukhtarev, S.G. Odulov: Proc. Opt. Photonics **213**-SPIE, 2–10 (1979)
8. M. Cronin-Golomb, J.O. White, B. Fischer, A. Yariv: Opt. Lett. **7**, 313–315 (1982)
9. Y.H. Ja: Opt. Quantum Electron. **15**, 529–538 (1983)
10. Y.H. Ja: Opt. Quantum Electron. **15**, 539–546 (1983)
11. Y. H. Ja: Appl. Phys. B **33**, 161–165 (1984)
12. R.P. Tewarson: Intern. J. Num. Methods Eng. **18**, 1313–1319 (1982)
13. J. Walsh: In *The State of the Art in Numerical Analysis*, ed. by D. Jacobs (Academic Press, London 1975) pp. 501–533
14. J.E. Key: Intern. J. Num. Methods Eng. **6**, 497–509 (1973)
15. R.P. Tewarson: BIT **20**, 223–232 (1980)
16. Y.H. Ja: Opt. Quantum Electron. **14**, 547–556 (1982)
17. J.P. Huignard, A. Marrakchi: Opt. Commun. **38**, 249–254 (1981)
18. A.A. Ballman: J. Cryst. Growth **1**, 37–40 (1967)
19. G.G. Douglas, R.N. Zitter: J. Appl. Phys. **39**, 2133–2135 (1968)
20. V.L. Vinetskii, N.V. Kukhtarev: Sov. J. Quantum Electron. **8**, 231–235 (1978)
21. Y.H. Ja: Opt. Quantum Electron. **16** (1984, in press)
22. R. Lytel: J. Opt. Soc. Am. B **1**, 91–94 (1984)

Note added in proof: The $O(h^7)$ method and the shooting scheme may be difficult to implement in the special case of optical multistability in DFWM. The initial-value and mapping techniques [22] can then be used to find the multiple solutions of the first-order nonlinear coupled-wave equations for DFWM.